JACS
JOURNAL OF THE AMERICAN CHEMICAL SOCIETY

Communication

pubs.acs.org/JACS

High-Pressure Chemistry of a Zeolitic Imidazolate Framework Compound in the Presence of Different Fluids

HPSTAR 239-2016

Junhyuck Im,[†] Narae Yim,[‡] Jaheon Kim,[‡] Thomas Vogt,[§] and Yongjae Lee*[,†,∥]

[†]Department of Earth System Sciences, Yonsei University, Seoul 03722, Korea

[‡]Department of Chemistry, Soongsil University, Seoul 06978, Korea

[§]NanoCenter and Department of Chemistry & Biochemistry, University of South Carolina, Columbia, South Carolina 29208, United States

[∥]Center for High Pressure Science & Technology Advanced Research (HPSTAR), Shanghai 201203, China

Supporting Information

ABSTRACT: Pressure-dependent structural and chemical changes of the zeolitic imidazolate framework compound ZIF-8 have been investigated using different pressure transmitting media (PTM) up to 4 GPa. The unit cell of ZIF-8 expands and contracts under hydrostatic pressure depending on the solvent molecules used as PTM. When pressurized in water up to 2.2(1) GPa, the unit cell of ZIF-8 reveals a gradual contraction. In contrast, when alcohols are used as PTM, the ZIF-8 unit cell volume initially expands by 1.2% up to 0.3(1) GPa in methanol, and by 1.7% up to 0.6(1) GPa in ethanol. Further pressure increase then leads to a discontinuous second volume expansion by 1.9% at 1.4(1) GPa in methanol and by 0.3% at 2.3(1) GPa in ethanol. The continuous uptake of molecules under pressure, modeled by the residual electron density derived from Rietveld refinements of X-ray powder diffraction, reveals a saturation pressure near 2 GPa. In non-penetrating PTM (silicone oil), ZIF-8 becomes amorphous at 0.9(1) GPa. The structural changes observed in the ZIF-8-PTM system under pressure point to distinct molecular interactions within the pores.

Zeolitic imidazolate frameworks (ZIFs) are crystalline porous materials assembled with tetrahedral metal centers and rigid imidazolate linkers, mimicking zeolites in terms of network types.[1] ZIF-8 has a sodalite-like topology and is among the most investigated ZIFs because it has a large surface area and an excellent chemical stability.[2] Potential practical applications of ZIF-8 also prompted the development of various synthetic methods,[3] including solventless high-pressure synthesis.[4] Due to the short and rigid imidazolate ligands coordinated to tetrahedral metal centers, the highly symmetric ZIF-8 structure is stiffer than other metal−organic frameworks.[5] However, recent studies reveal the inherent flexibility of ZIF-8 under high pressure.[6−8] For example, when a mixture of ethanol and methanol is used as pressure transmitting media (PTM), the 2-methylimidazolate ligand connecting two Zn ions in ZIF-8 rotate near 1.5 GPa, leading to an increase of the pore volume followed by a transition to a high-pressure phase due to a selective and continuous pressure-induced insertion (PII) of methanol molecules.[7] This change of the imidzolate orientation has been also observed in theoretical calculations.[9] Water intrusion-extrusion experiments show that the particle size and shape affect structural deformation in ZIF-8 up to 40 MPa.[10] IR spectroscopy studies without any PTM show that ZIF-8 is compressed reversibly below 1.6 GPa,[11] and CO_2 molecules interact with the imidazolate C═C bonds near 0.8 GPa, leading to pressure-induced enhanced CO_2 storage.[12]

ZIFs are predicted to reveal a rich chemistry at high pressures considering the accumulated findings of their inorganic counterparts, zeolites. For example, a small-pore zeolite, natrolite, shows discontinuous and reversible pressure-induced hydration,[13] pressure-induced amorphization (PIA),[14] and discontinuous PII of Ar, Kr, or Xe or molecules such as CO_2 into the pores.[15−23] Water can be inserted at room temperature, whereas CO_2 and other entities often require additional heating.[20−23] Reversible[16] or irreversible PII can produce new materials. Xenon atoms can be inserted irreversibly into the expanded pores of Ag-exchanged natrolite using moderate pressure and temperature at 1.7(1) GPa and 250(2) °C.[23] Volume changes of ZIF-8 under pressure are known to be of 1−2%,[7] whereas natrolites are up to 20%[13] due to the displacive rotations of structural subunits (T_5O_{10} units). However, we show here that in contrast to natrolite, in ZIF-8 both continuous and discontinuous PII occur. While distinct high-pressure phases with well-defined stoichiometries and bulk moduli are observed in natrolites,[17,22] the regions of unit cell expansion during continuous PII of molecules under pressure create an ensemble of different phases in ZIF-8.

Here, we report in situ high-resolution synchrotron X-ray powder diffraction (XRD) investigations revealing unique guest-dependent structural modifications of ZIF-8 under high pressure using water, methanol, ethanol as a hydrostatic PTM, where molecules can be inserted into the ZIF-8 framework and silicone oil as a non-penetrating fluid. As-synthesized ZIF-8 (labeled ZIF-8) was prepared according to the literature[3b] and pristine ZIF-8 has a cubic space group $I\bar{4}3m$ with a = 17.031(2) Å and V = 4940(2) Å^3 (Figure 1). High-pressure experimental conditions and results are listed in Table S1. The synchrotron XRD patterns measured in various fluids up to 4 GPa are presented in Figure 2. The normalized volume changes in the

Received: July 18, 2016
Published: August 30, 2016

DOI: 10.1021/jacs.6b07374
J. Am. Chem. Soc. 2016, 138, 11477−11480

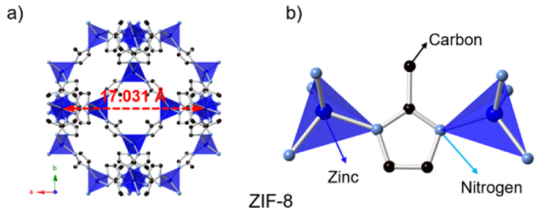

Figure 1. Structural models of (a) a sodalite cage and (b) two Zn tetrahedrons linked by 2-methylimidazolate in ZIF-8. Hydrogen atoms are omitted for simplicity.

unit cell are displayed in Figure 3. In addition, the accompanied changes in the size of a hexagonal window are provided in Figure S1.

To ensure reproducible hydrostatic conditions at GPa pressures, various fluid pressure transmitting media are commonly used.[24] ZIF-8 was sealed with water as PTM in the sample chamber of a diamond anvil cell and subjected to pressures up to 2.2(1) GPa. As shown in Figure 2a, the initial powder diffraction pattern of ZIF-8 reveals a slight expansion due to an uptake of water (ZIF-8-$W_{(1-x)}$) followed by a contraction of the system. For ZIF-8-$W_{(1-x)}$, the initial expansion of the unit cell volume was ca. 0.2% up to 0.3(1) GPa. Subsequent Rietveld analyses revealed that despite a linear compressibility, ZIF-8-$W_{(1-x)}$ was actually composed of

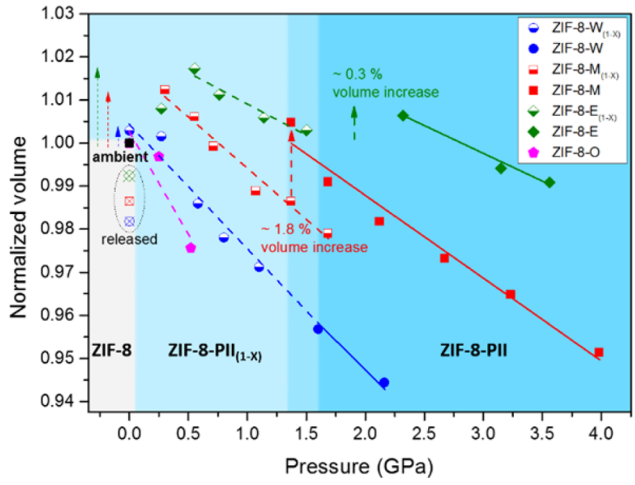

Figure 3. Pressure-dependent changes of the normalized unit cell volume of ZIF-8 in water (W), methanol (M), ethanol (E), and silicone oil PTM (O). Estimated standard deviations are smaller than the size of each symbol.

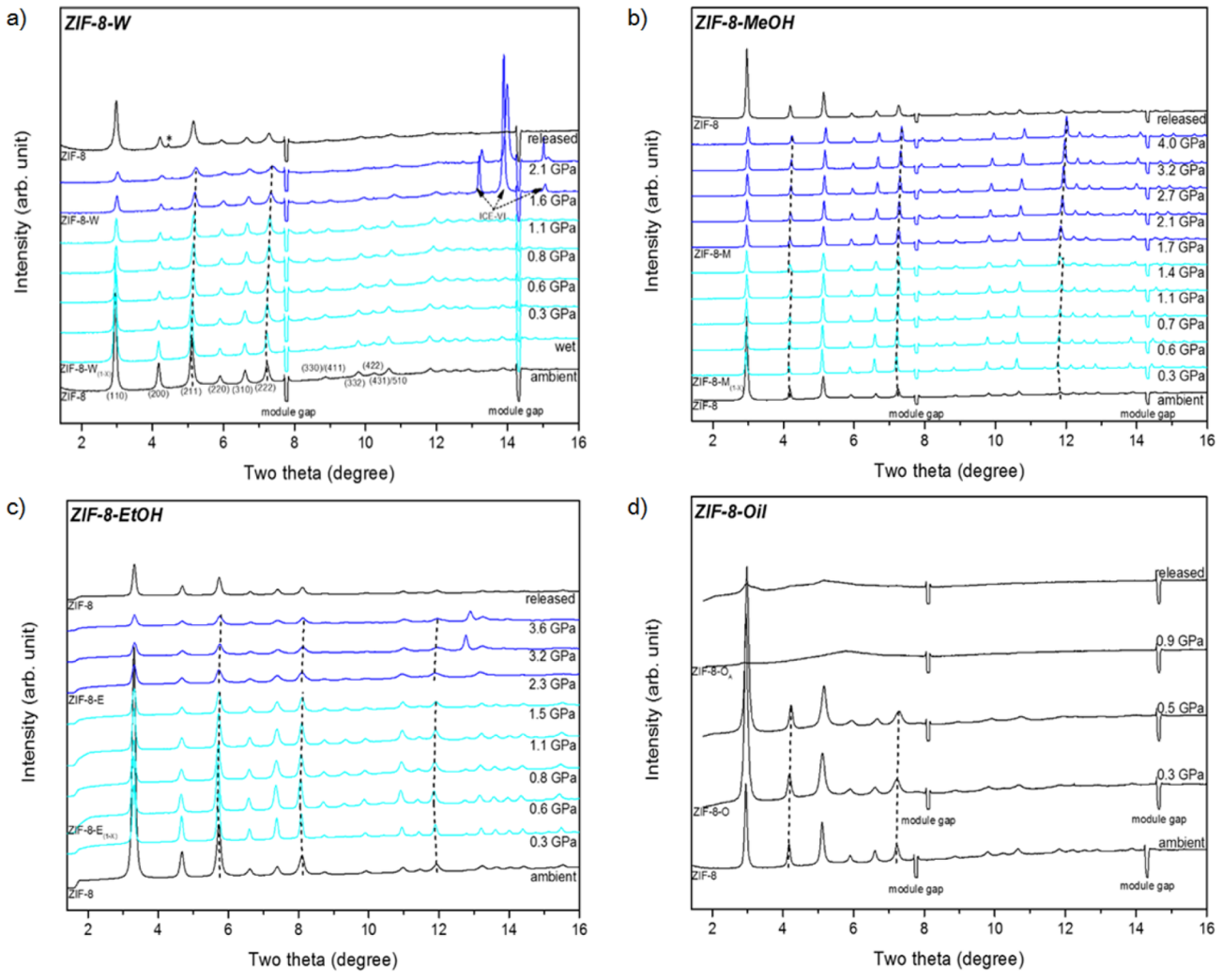

Figure 2. Synchrotron X-ray powder diffraction patterns of ZIF-8: pressure-dependent patterns in (a) water, (b) methanol, (c) ethanol, and (d) silicone oil.

DOI: 10.1021/jacs.6b07374
J. Am. Chem. Soc. 2016, 138, 11477−11480

numerous distinct phases with different H_2O contents as displayed by the dotted lines in Figures 2a and 3. A compressibility (β) of 0.03143 GPa^{-1} was calculated for the ensemble of ZIF-8-$W_{(1-x)}$ phases. However, one should not calculate a bulk modulus on the basis of these data; rather, the intrinsic bulk modulus for each phase needs to be determined by collecting individual XRD data in silicone oil (vide infra). Above 1.6(1) GPa, the pores of ZIF-8 are completely filled with H_2O due to PII and a single ZIF-8-W phase is now present (Figure 4a). As expected based on the water−ice phase

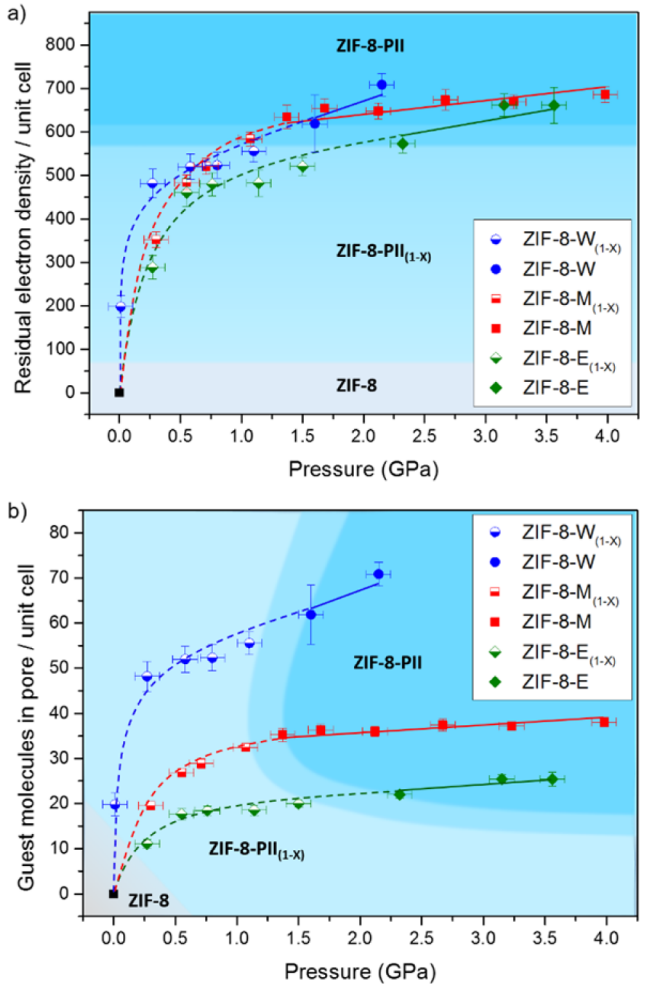

Figure 4. (a) Calculated residual electron density as pressure increases. (b) Pressure-induced insertion of guest molecules into the pores of ZIF-8 in water (W), methanol (M), and ethanol (E) PTM as pressure increases.

diagram, the inserted H_2O crystallized near 1.6 GPa to an ice-VI phase accompanied by a significant broadening of the diffraction peaks of ZIF-8-W (Figure 2a). This broadening can indicate the onset of non-hydrostatic conditions or a partial decomposition of the ZIF-8 framework. During pressure increase, a tiny undefined peak (asterisk in Figure 2a) appeared next to the (200) peak but could not be indexed commensurately with the lattice of ZIF-8-W; we believe this to be a spurious peak from the experimental setup.

Using methanol as PTM, the changes in the measured XRD patterns indicated clearly the presence of three distinct pressure regions designated as as-synthesized ZIF-8, ZIF-8-$M_{(1-x)}$ between 0.3(1) and 1.7(1) GPa, and ZIF-8-M above 1.4(1) GPa (Figure 2b). The unit cell volume of ZIF-8 expands by ca. 1.7% when pressurized to 0.3(1) GPa. Subsequently, the unit cells of the ZIF-8-$M_{(1-x)}$ phases contract until a pressure of 1.4(1) GPa is reached. At this pressure, a ZIF-8-M phase begins to form, and both ZIF-8-$M_{(1-x)}$ and ZIF-8-M phases coexist until 1.7(1) GPa. As shown in Figure 4, the constant methanol content above 1.4(1) GPa suggests that a single ZIF-8-M phase is present in the pressure range up to 4.0(1) GPa. This phase has a bulk modulus of 40(2) GPa. The unit cell volume of ZIF-8 increased by 1.8% at 1.4(1) GPa in ZIF-8-M (see dashed lines in Figures 2b and 3).

When using ethanol as PTM, four distinct pressure regions are identified on the basis of the XRD patterns shown in Figure 2c: ZIF-8, an intermediate phase at 0.3(1) GPa, the first high-pressure phase between 0.6(1) and 1.5(1) GPa (ZIF-8-$E_{(1-x)}$), and the second high-pressure phase between 2.3(1) and 3.6(1) GPa (ZIF-8-E). The initial expansion of the unit cell volume observed in ZIF-8 systematically increases from ambient (in *water*) to 0.3(1) (in *methanol*) to 0.6(1) GPa (in *ethanol*, Figure 3). The threshold pressure for the emergence of a high-pressure single phase increases from 1.4(1) (in *methanol*) to 2.3(1) GPa (in *ethanol*). The compressibility of the ZIF-8-$E_{(1-x)}$ phase was calculated to be 0.01754 GPa^{-1}. The formation of the second high-pressure phase (labeled ZIF-8-E) was accompanied by the unit cell volume expansion by ca. 0.3% at 2.3(1) GPa. The bulk modulus of the ZIF-8-E phase is with 73(4) GPa, the largest observed in this work. The compressibility, bulk moduli of high-pressure phases and the pressure range where we observe PII in ZIF-8 are similar to those observed by others[7,25] and other MOFs such as MIL-47(V).[26] The unit cell volumes of the ZIF-8 phases after pressure release in different pore-penetrating PTM were ca. 1.3−1.8% smaller than that of as-synthesized ZIF-8 and remained in this state. The diffraction pattern of the ZIF-8 sample after the experiment using ethanol as PTM revealed smaller intensities and broader peaks, indicating a higher level of disorder than before the experiment.

In the presence of non-penetrating silicone oil, the diffraction peak shifts indicated by the dashed lines in Figure 2d reveal an initial contraction of the unit cell volume up to 0.5(1) GPa (Figure 3, labeled ZIF-8-O). The bulk modulus of ZIF-8-O with 20(5) GPa is the smallest measured in our experiments. Above 0.9(1) GPa, the diffraction peaks disappear, indicating PIA. The amorphous phase ZIF-8-O_A was retained after exposure to ambient pressure, and no re-crystallization to the original phase was found later. Compared to the ZIF-8 phases in contact with pore-penetrating PTM, there was no evidence of any unit cell volume expansion in the presence of non-penetrating silicone oil.

Since the PII process is similar when using methanol or ethanol as PTM, the different XRD patterns may be attributed to the molecular size difference between the two alcohols. Contrary to alcohols, water molecules would interact more weakly with the hydrophobic ZIF surfaces, and therefore the ice-VI formation at 1.6 GPa seems to induce the structural change of ZIF-8. Previous high-pressure single-crystal studies of ZIF-8 reported a selective PII of methanol from the PTM, which involved an expansion of the unit cell volume by ca. 1.7% near 1.5 GPa concomitant with a pore opening due to the rotation of 2-methylimidazolate ligand.[7] In addition to confirming this structural distortion, we could establish the occurrence of a continuous PII in ZIF-8-$M_{(1-x)}$ and determined the bulk modulus of the high-pressure phase ZIF-8-M. Moreover, we have shown that the stepwise expansion of the

DOI: 10.1021/jacs.6b07374
J. Am. Chem. Soc. 2016, 138, 11477−11480

ZIF-8 unit cell volume depends on the molecular species present in the PTM. The PTM-dependent bulk moduli of the high-pressure single phases were also confirmed. When non-penetrating silicone oil was used as PTM, we found a much lower bulk modulus (20(5) GPa) than those observed under other PTM conditions.

The residual electron densities in the pores of ZIF-8 in the presence of different pore-penetrating fluids were examined using difference Fourier density maps provided by the GSAS program (Figure 4a and Table S2). Due to PII, the electron densities in the pores increased with pressure. Plots of the residual electron density against pressure produced type-I isotherms with a saturation value near 600 electrons per unit cell (Figure 4a). These electron densities were converted to numbers of inserted molecules as shown in Figure 4b. Based on the work by Moggach and co-workers,[7] the pore volume of ZIF-8 was estimated to be 2450 Å^3, and those of ZIF-8 under pressure were between 2215 and 2504 Å^3 for water, 2250 and 2552 Å^3 for methanol, and 2430 and 2560 Å^3 for ethanol. Accordingly, using the approximate molecular volumes of H_2O (29.9 Å^3), CH_3OH (67.0 Å^3), and C_2H_5OH (97.0 Å^3), the maximums number of guest molecules in ZIF-8 were calculated to be in the range of 74−84 (water), 34−38 (methanol), and 25−26 (ethanol) (Figure 4b).

In summary, we have explored the compression behavior of ZIF-8 in the presence of different fluids and found a clear dependence of the magnitude of pressure-induced insertion and associated volume expansions on the size of molecules. The degree of initial expansion, the onset pressure of PII, and bulk moduli where single phases are present scale with the size of the PTM molecules. Upon pressure increase under water, methanol, and ethanol, the electron density within the pores of ZIF-8 increases, indicating both continuous and discontinuous PII. Our studies show that continuous PII results in an ensemble of high-pressure phases where a bulk modulus cannot be assigned on the basis of a single compressibility experiment. These host−guest interactions have to be taken into account, and other methods need to be employed to determine the intrinsic mechanical behavior of ZIF-8 or any of its high-pressure phases created by continuous PII.[27] Finally, our results suggest that future explorations of the high-pressure chemistry of ZIFs and other MOFs should probe molecular diffusion and/or chemical reactions in pores under high pressure.

■ ASSOCIATED CONTENT

Supporting Information

The Supporting Information is available free of charge on the ACS Publications website at DOI: 10.1021/jacs.6b07374.

Experimental details, Figure S1, and Tables S1 and S2 (PDF)

■ AUTHOR INFORMATION

Corresponding Author

*yongjaelee@yonsei.ac.kr

Notes

The authors declare no competing financial interest.

■ ACKNOWLEDGMENTS

This work was supported by the Global Research Laboratory (NRF-2009-00408) and National Research Laboratory (NRF-2015R1A2A1A01007227) programs of the Korean Ministry of Science, ICT and Planning (MSIP). We also thank the supports by NRF-2016K1A4A3914691 and NRF-2016K1A3A7A09005244 grants. Experiments using the synchrotrons were supported by PAL and the Collaborative Access Program of SSRL.

■ REFERENCES

(1) Park, K. S.; Ni, Z.; Côté, A. P.; Choi, J. Y.; Huang, R.; Uribe-Romo, F. J.; Chae, H. K.; O'Keeffe, M.; Yaghi, O. M. *Proc. Natl. Acad. Sci. U. S. A.* **2006**, *103*, 10186.

(2) Zhang, C.; Koros, W. J. *J. Phys. Chem. Lett.* **2015**, *6*, 3841.

(3) (a) Lee, Y.-R.; Jang, M.-S.; Cho, H.-Y.; Kwon, H. J.; Kim, S.; Ahn, W.-S. *Chem. Eng. J.* **2015**, *271*, 276. (b) Cravillon, J.; Münzer, S.; Lohmeier, S.-J.; Feldhoff, A.; Huber, K.; Wiebcke, M. *Chem. Mater.* **2009**, *21*, 1410.

(4) Paseta, L.; Potier, G.; Sorribas, S.; Coronas, J. *ACS Sustainable Chem. Eng.* **2016**, *4*, 3780.

(5) (a) Morris, W.; Stevens, C. J.; Taylor, R. E.; Dybowski, C.; Yaghi, O. M.; Garcia-Garibay, M. A. *J. Phys. Chem. C* **2012**, *116*, 13307. (b) Férey, G.; Serre, C. *Chem. Soc. Rev.* **2009**, *38*, 1380.

(6) Chapman, K. W.; Halder, G. J.; Chupas, P. J. *J. Am. Chem. Soc.* **2009**, *131*, 17546.

(7) Moggach, S. A.; Bennett, T. D.; Cheetham, A. K. *Angew. Chem., Int. Ed.* **2009**, *48*, 7087.

(8) Zhao, P.; Bennett, T. D.; Casati, N. P. M.; Lampronti, G. I.; Moggach, S. A.; Redfern, S. A. T. *Dalton T.* **2015**, *44*, 4498.

(9) (a) Fairen-Jimenez, D.; Moggach, S. A.; Wharmby, M. T.; Wright, P. A.; Parsons, S.; Düren, T. J. *J. Am. Chem. Soc.* **2011**, *133*, 8900. (b) Zhang, L.; Hu, Z.; Jiang, J. *J. Am. Chem. Soc.* **2013**, *135*, 3722.

(10) Khay, I.; Chaplais, G.; Nouali, H.; Marichal, C.; Patarin, J. *RSC Adv.* **2015**, *5*, 31514.

(11) Hu, Y.; Kazemian, H.; Rohani, S.; Huang, Y.; Song, Y. *Chem. Commun.* **2011**, *47*, 12694.

(12) Hu, Y.; Liu, Z.; Xu, J.; Huang, Y.; Song, Y. *J. Am. Chem. Soc.* **2013**, *135*, 9287.

(13) (a) Seoung, D.; Lee, Y.; Kao, C. C.; Vogt, T.; Lee, Y. *Chem. - Eur. J.* **2013**, *19*, 10876. (b) Seoung, D.; Lee, Y.; Kao, C. C.; Vogt, T.; Lee, Y. *Chem. Mater.* **2015**, *27*, 3874.

(14) Hwang, G. C.; Shin, T. J.; Blom, D. A.; Vogt, T.; Lee, Y. *Sci. Rep.* **2015**, *5*, 15056.

(15) Hazen, R. M. *Science* **1983**, *219*, 1065.

(16) Gillet, P.; Malézieux, J. M.; Itié, J. P. *Am. Mineral.* **1996**, *81*, 651.

(17) Lee, Y.; Vogt, T.; Hriljac, J. A.; Parise, J. B.; Hanson, J. C.; Kim, S. J. *Nature* **2002**, *420*, 485.

(18) Lee, Y.; Hriljac, J. A.; Parise, J. B.; Vogt, T. *Am. Mineral.* **2005**, *90*, 252.

(19) Lee, Y.; Hriljac, J. A.; Vogt, T. *J. Phys. Chem. C* **2010**, *114*, 6922.

(20) Lee, Y.; Liu, D.; Seoung, D.; Liu, Z.; Kao, C. C.; Vogt, T. *J. Am. Chem. Soc.* **2011**, *133*, 1674.

(21) Lee, Y.; Lee, Y.; Seoung, D.; Im, J. H.; Hwang, H. J.; Kim, T. H.; Liu, D.; Liu, Z.; Lee, S. Y.; Kao, C. C.; Vogt, T. *Angew. Chem., Int. Ed.* **2012**, *51*, 4848.

(22) Lee, Y.; Seoung, D.; Jang, Y. N.; Vogt, T.; Lee, Y. *Chem. - Eur. J.* **2013**, *19*, 5806.

(23) Seoung, D.; Lee, Y.; Cynn, H.; Park, C.; Choi, K.-Y.; Blom, D. A.; Evans, W. J.; Kao, C.-C.; Vogt, T.; Lee, Y. *Nat. Chem.* **2014**, *6*, 835.

(24) Klotz, S.; Chervin, J. C.; Munsch, P.; Le Marchand, G. *J. Phys. D: Appl. Phys.* **2009**, *42*, 075413.

(25) Graham, A. J.; Allan, D. R.; Muszkiewicz, A.; Morrison, C. A.; Moggach, S. A. *Angew. Chem., Int. Ed.* **2011**, *50*, 11138.

(26) Im, J.; Seoung, D.; Hwang, G. C.; Jun, J. W.; Jhung, S. H.; Kao, C.-C.; Vogt, T.; Lee, Y. *Chem. Mater.* **2016**, *28*, 5336.

(27) Su, Z.; Miao, Y.-R.; Mao, S.-M.; Zhang, G.-H.; Dillon, S.; Miller, J. T.; Suslick, K. S. *J. Am. Chem. Soc.* **2015**, *137*, 1750−1753.

DOI: 10.1021/jacs.6b07374
J. Am. Chem. Soc. 2016, 138, 11477−11480